# Real and causal hysteresis elements

Kevin J. Parker[a)]

*Department of Electrical & Computer Engineering, University of Rochester, Hopeman Engineering Building 203, P.O. Box 270126, Rochester, New York 14627-0126*

Hysteresis is a phenomenon that has been observed across many different materials and situations. Under small-amplitude cyclical motion, classical hysteresis designates a constant loss per cycle over a wide range of frequencies. This is also consistent with an increase in losses or attenuation with frequency that is strictly proportional to the first power of frequency. Unfortunately, the classical (and simple) frequency domain description of hysteresis does not result in a real and causal impulse response, and therefore is not useful for predicting laboratory results. This problem has led to many errors as well as other more fruitful approaches over the years. The frequency domain requirements for hysteresis are re-examined and it is demonstrated that there is a family of solutions that provide real and causal impulse responses over some extended frequency range. The family is conveniently divided into highpass, lowpass, and bandpass causal systems. These are populated by closed form analytical solutions which can be applied to the prediction of motion and waves in hysteretic materials and systems. © *2014 Acoustical Society of America.*
[http://dx.doi.org/10.1121/1.4876183]

## I. INTRODUCTION

There is a long standing recognition that in a variety of situations, from the movement of soil to waves in metals, the energy dissipation during cyclical motion can increase as the first power of frequency, over an extended frequency range (Kimball and Lovell, 1927; Wegel and Walther, 1935; Mason and McSkimin, 1947). That implies that the losses per cycle are constant over many octaves, and this behavior has been called hysteresis, a hypothetical loss element or process that creates a constant phase lag between stress and strain over all frequencies (Theodorsen and Garrick, 1940; Mason, 1950). In the early 20th century, hysteresis effects were thought to be prominent across a diverse range of materials and conditions. Kimball and Lovell (1927) at GE Labs reported that hysteresis was found "over a considerable frequency range" and "for a number of solids of very different physical properties." Later, Mason stated (Mason and McSkimin, 1947) that "the component proportional to frequency is the same as observed for most metals and solid materials at low frequencies, and indicates the presence of an elastic hysteresis." The issue of hysteresis is of continuing importance in a diverse set of areas, including earthquake motion and damping of structures, and, possibly in shear wave propagation in biomedical tissues (Makris and Zhang, 2000; Nakamura, 2007; Carstensen and Parker, 2014).

Unfortunately, there remains a fundamental and irreconcilable difference between the classical, idealized frequency domain description of hysteresis and practical, causal time domain realizations, and this problem has been the subject of numerous papers over the past decade.

The Kramers–Kronig relationship links and constrains the relationship between the real and imaginary parts of a transfer function in the frequency domain, based on the constraint that the impulse response of a material is a real and causal function (Nachman *et al.*, 1990; Szabo and Wu, 2000; Nasholm and Holm, 2011). Nevertheless, the most straightforward description of a constant phase shift in the frequency domain is simply a transfer function with constant real and imaginary parts, as given by Mason (1950). However, if formulated to be consistent with a real impulse response, the corresponding impulse response is an acausal $1/t$ function (valid for both positive and negative time $t$), and this well-known transform pair is related to the Hilbert transform (Crandall, 1963; Bracewell, 1965; Crandall, 1970).

Thus, there is a problem reconciling a real, causal impulse response for a hysteresis loss element while simultaneously maintaining the classical "constant real and imaginary" formulation in the frequency domain.

To address this problem, a number of researchers have taken different approaches. Inaudi and Kelly (1995) proposed an iterative technique in the time domain to approach a realizable hysteretic element. Their introduction is also useful as a review of the many incorrect approaches and *ad hoc* formulations that were proposed in the past as researchers grappled with the fundamentally irreconcilable difference between the simple Mason complex constant (in the frequency domain) and the need for a real and causal response in the time domain. Other recent formulations include Nakamura (2007) who introduced a discrete time approximation with up to 18 terms. Makris and Zhang (2000) proposed a real and causal time domain function, however, it had a singularity at zero frequency. They compared this result with a much earlier result from Biot (1958) which has a storage modulus that, at high frequencies, increases as $\log(\omega)$, where $\omega$ is the frequency. The hysteresis

---

[a)]Author to whom correspondence should be addressed. Electronic mail: kevin.parker@rochester.edu

loss at high frequencies is essentially constant, independent of frequency (Caughey, 1962; Inaudi and Kelly, 1995). The paper by Biot is noteworthy as a contribution since it opens the suggestion that perhaps the hysteresis model could be approximated by a nearly constant modulus over a limited frequency range. This loosening of the definition is key to achieving a working synthesis. Unfortunately, Biot's contribution is given as a "short remark on the nature of solid friction" at the end of a highly theoretical paper on linear thermodynamics. As such, its inference may have been underappreciated for many years.

In this paper we re-examine the fundamental requirements for hysteresis and causality, and demonstrate that there is a diverse set of continuous, real, causal analytic functions that provide the hysteresis behavior over a range of observable frequencies, but within a set of constraints that permit only an approximation to the classical formulation of constants.

## II. THEORY

In terms of signal theory (Papoulis, 1987), any real and causal signal $T(t)$ can be considered to be the sum of two real functions: $T(t) = E(t) + O(t)$ representing even and odd functions of time, respectively. These two are identical for $t > 0$ but are opposite for $t < 0$ and therefore the sum is causal. Their Fourier transforms are also real and even, and imaginary and odd, respectively. Specifically,

$$\Im\{T(t)\} = R(\omega) + jX(\omega), \tag{1}$$

where $\Im\{\ \}$ denotes the Fourier transform operation, and because of the even, odd properties,

$$R(\omega) = 2\int_0^\infty E(t)\cos(\omega t)dt, \tag{2}$$

and $R(\omega)$ is an even function of $\omega$; and

$$X(\omega) = -2\int_0^\infty O(t)\sin(\omega t)dt \tag{3}$$

and $X(\omega)$ is an odd function of $\omega$.

Furthermore, since the two functions are equal for $t > 0$, it can be shown then that as a consequence, the cosine Fourier transform of the even part must equal the sine Fourier transform of the odd part. Specifically,

$$T(t) = 2E(t) = 2O(t) \quad \text{for} \quad t > 0. \tag{4}$$

Thus, using the inverse transform relations,

$$T(t) = \frac{2}{\pi}\int_0^\infty R(\omega)\cos(\omega t)d\omega$$
$$= -\frac{2}{\pi}\int_0^\infty X(\omega)\sin(\omega t)d\omega \quad \text{for} \quad t > 0. \tag{5}$$

This is another way of saying that the real and imaginary parts of the frequency domain, $R(\omega)$ and $X(\omega)$, are linked and dependent for a causal function, a relationship which is alternatively captured in Kramers–Kroning relations.

Adopting Mason's (1950) formulation for strain $S$ and stress $T$ in a solid material with hysteresis $H$ and elastic constant $K$ under plane wave conditions we begin with the frequency domain equation

$$T(\omega) = (K + jH)S(\omega), \tag{6}$$

where the purely elastic $K$ plus hysteretic $H$ elements are independent of frequency $\omega$. We see immediately that the hysteretic term $H$ (which comprises the imaginary component) must be made an odd function of frequency [so as to correspond to a real transfer function following Eq. (3)], and so must take the form $jH\,\text{Sign}(\omega)$. Thus,

$$T(\omega) = (K + jH\,\text{Sign}(\omega))S(\omega). \tag{7}$$

We now have a transfer function whose real part is even and whose imaginary part is odd. This is one requirement for causality. But can we also satisfy the Fourier cosine and Fourier sine equality requirement [Eq. (5)] with constant functions of frequency for both $K$ and $H$? The answer is no if we insist on constant $K$ and $H$ over all frequencies, since the Fourier cosine transform of a constant yields an impulse in time, whereas the Fourier sine transform of a constant yields a $1/t$ function, hence we cannot use two constants simultaneously to satisfy the basic requirements of a real, causal response. In other words, if we examine the impulse response of the transfer function of Eq. (7), then $S(\omega) = 1$ and $T(\omega) = K + jH\,\text{Sign}[\omega]$. Then, examining Eq. (5) with $R(\omega) = K$ and $X(\omega) = H$, we have

$$T(t) = \frac{2}{\pi}\int_0^\infty K\cos(\omega t)d\omega = 2K\delta(t) \tag{8}$$

but, furthermore,

$$T(t) = -\frac{2}{\pi}\int_0^\infty H\sin(\omega t)d\omega = \frac{2H}{\pi t}. \tag{9}$$

These are not equal for any constant value of $K, H$ except for the trivial case where $H = K = 0$. Thus, something has to vary in Eq. (7) in order to establish a real and causal impulse response.

However, following Biot (1958), if we allow for some variation at extremely low frequencies, then we can perhaps find solutions that do provide a constant phase shift (or a constant loss per cycle) over a very wide frequency range, and at the same time provide for a real and causal response to an applied impulse of stress. Thus, we designate the requirements for limited hysteresis over an observable frequency range $\omega_{\min} < \omega < \omega_{\max}$, where $\omega_{\min} \ll \omega_{\max}$ as

$$T(\omega) = (K(\omega) + jH(\omega))S(\omega), \tag{10}$$

and where

$$H(\omega) \cong H_0 \quad \text{for} \quad \omega_{\min} < \omega < \omega_{\max},$$

and where $K(\omega)$ is an even function of $\omega$, $H(\omega)$ is odd.

Kevin J. Parker: Real and causal hysteresis elements

## A. Conditions for limited hysteresis

A limitation of the formulation comes from examining the energy loss per cycle in hysteresis in sinusoidal steady state at some frequency $\omega_0$. Starting with Eq. (10), let $S = S_0 \cos(\omega_0 t) = \mathrm{Re}[S_0 e^{j\omega_0 t}]$, then

$$
\begin{aligned}
T &= \mathrm{Re}\left[S_0(K + jH)e^{j\omega_0 t}\right] \\
&= S_0(K^2 + H^2)^{1/2}\cos(\omega_0 t + \theta),
\end{aligned} \tag{11}
$$

where $\theta = \arctan\left[H(\omega_0)/K(\omega_0)\right]$. Along the cyclical path of stress and strain the energy $E$ dissipated is given by

$$
\begin{aligned}
dE &= T\,dS = T\frac{dS}{dz}dz \\
&= -S_0(K^2 + H^2)^{1/2}\cos(z + \theta)S_0\sin(z)dz \\
&= -S_0^2(K^2 + H^2)^{1/2}\cos(z + \theta)\sin(z)dz
\end{aligned} \tag{12}
$$

and the total energy dissipated per cycle is

$$
\begin{aligned}
E &= \int_0^{2\pi} dE = -S_0^2(K^2 + H^2)^{1/2}\int_0^{2\pi}\cos(z + \theta)\sin(z)dz \\
&= +\pi S_0^2(K^2 + H^2)^{1/2}\sin[\theta].
\end{aligned} \tag{13}
$$

Note that $\sin[\theta] = \sin[\arctan[H/K]] = H/\sqrt{K^2 + H^2}$. Thus,

$$
E(\omega) = \pi S_0^2 H(\omega), \tag{14}
$$

indicating that if $H(\omega)$ is constant then the resulting energy loss per cycle will be constant over a frequency range. However, this is only true if strain $S_0$ is treated as the independent variable and also held strictly constant over the frequency range. This could be accomplished experimentally with conventional load cell equipment; however it is not generally the case, especially in wave propagation. Thus the inference of Eq. (14) that hysteresis will be exhibited only if $H(\omega)$ is constant is restricted to special circumstances and will be called "limited hysteresis." Even in these restricted circumstances—with $S_0$ and $H(\omega)$ constant—causality requirements will specify $K(\omega)$ to be a non-constant, so the idealization of Eq. (6) is not realizable.

## B. Conditions for strict hysteresis

Under wave propagation, the requirements for hysteresis are more stringent since we now require the attenuation (the imaginary part of the wave number) to increase linearly with frequency. This constrains the material properties. As one example, in sinusoidal steady state plane shear wave propagation in an isotropic elastic material with losses, the general relationship is

$$
T(\omega) = \mu S(\omega). \tag{15}
$$

$\mu$ is the shear modulus and the shear wave speed $c_s = \sqrt{\mu/\rho}$, where $\rho$ is the density. Assuming that $\mu$ can be described as $\mu(\omega) = K(\omega) + jH(\omega)$, then the complex wave number is

$$
k = \frac{\omega}{c_s} = \beta - j\alpha = \frac{\omega}{\sqrt{\dfrac{K(\omega) + jH(\omega)}{\rho}}}. \tag{16}
$$

Here, $k$ is the wavenumber with real ($\beta$) and imaginary ($\alpha$) parts (Blackstock, 2000). The attenuation coefficient $\alpha$ of a propagating wave will therefore be a function of frequency depending on $K(\omega)$ and $H(\omega)$. Expanding on the real and imaginary parts of Eq. (16) we have

$$
\beta = \omega\sqrt{\frac{\rho}{K^2 + H^2}}\left[\frac{1}{2}\left(1 + \frac{1}{\sqrt{1 + \dfrac{H^2}{K^2}}}\right)\right]^{1/2} \tag{17}
$$

and the wave speed

$$
c = \sqrt{\sqrt{\frac{K^2 + H^2}{\rho}}\left[\frac{1}{2}\left(1 + \frac{1}{\sqrt{1 + \dfrac{H^2}{K^2}}}\right)\right]^{-1/2}} \tag{18}
$$

and the absorption coefficient

$$
\begin{aligned}
\alpha &= \omega\sqrt{\frac{\rho}{\sqrt{K^2 + H^2}}}\left[\frac{1}{2}\left(1 - \frac{1}{\sqrt{1 + \dfrac{H^2}{K^2}}}\right)\right]^{1/2} \\
&= \frac{\omega}{c}\sqrt{\frac{1 - \dfrac{1}{\sqrt{1 + \dfrac{H^2}{K^2}}}}{1 + \dfrac{1}{\sqrt{1 + \dfrac{H^2}{K^2}}}}}.
\end{aligned} \tag{19}
$$

As a limiting case, for $K \gg H$,

$$
c \to \sqrt{\frac{K}{\rho}} \tag{20}
$$

and

$$
\alpha \to \frac{\omega}{2c}\frac{H}{K}. \tag{21}
$$

However, for $K \ll H$,

$$
c \to \sqrt{\frac{2H}{\rho}}, \tag{22}
$$

$$
\alpha \to \omega\sqrt{\frac{\rho}{2H}} = \frac{\omega}{c}, \tag{23}
$$

and

$$
\alpha\lambda \to 2\pi. \tag{24}
$$

Considering Eqs. (17)–(19), we see that if $K^2(\omega) + H^2(\omega) = $ constant, and if $H(\omega)/K(\omega) = $ constant, then $c$ will be independent of frequency while $\alpha$ will be linearly proportional to frequency. This behavior has been

traditionally associated with waves in a hysteretic material since Mason (Mason and McSkimin, 1947; Mason, 1950). However, this behavior can only be observed in a passive medium if both $H(\omega)$ and $K(\omega)$ are approximately constant over some extended frequency range. We call this the "strict hysteresis" criterion and have already noted that achieving the strict criterion, $H(\omega) = H_0$ and $K(\omega) = K_0$, over all frequencies is not possible with real, causal functions.

## C. Realizations over frequency bands

Considering our framework for hysteresis over an observable frequency range $\omega_{min} < \omega < \omega_{max}$, we note that causal hysteretic functions (initially we examine "limited" hysteresis functions) can be classified conveniently into three subgroups.

(1) Highpass causal hysteresis functions: $H(\omega) \approx H_0$ for $\omega_{min} < \omega < \infty$ (essentially $\omega_{max} \to \infty$).
(2) Lowpass causal hysteresis functions: $H(\omega) \approx H_0$ for $0 < \omega < \omega_{max}$ (essentially $\omega_{min} \to 0$).
(3) Bandpass causal hysteresis functions: $H(\omega) \approx H_0$ for $\omega_{min} < \omega < \omega_{max}$; $H(\omega) \to 0$ otherwise.

## III. RESULTS

By reference to tables of Fourier transforms (Bracewell, 1965) and with the help of the MATHEMATICA computation system (Wolfram Research, Champaign, IL, USA, whose notation for functions is used in all following equations), a number of functions can be found as candidates for $K(\omega) + jH(\omega)$ and its real, causal transform $h(t)$.

The list below is not exhaustive; it simply presents some candidates to illustrate the scope of the family of solutions. We begin with an examination of some more obvious functions that, upon closer inspection, have serious problems in terms of practicality.

F1: The function

$$(1/t)\text{UnitStep}[t] \tag{25}$$

has the Fourier transform of

$$\frac{-2\gamma - 2\log[\text{Abs}[\omega]] + i\pi\,\text{Sign}[\omega]}{2\sqrt{2\pi}}, \tag{26}$$

where $\gamma$ is Euler's constant. This is the simplest of the functions that are causal yet related to Mason's model and with the idealized constant $H(\omega) = 1/2\sqrt{\pi/2}\,\text{Sign}[\omega]$ from $0 < \omega < \infty$. However, because of the slow asymptotic decay of $1/t$ as $t \to \infty$, $K(0)$ is infinite. This means that the function represents a material with stiffness approaching infinity at very low frequencies. Furthermore, the real part $K(\omega)$ goes negative, whereas passive, non-resonant materials will have positive $K$. Finally, the singularity at $t = 0$ is impossible to realize experimentally, and is difficult to deal with in convolution operations. Thus, while $\text{UnitStep}[t]/t$ has the ideal $H$ suggested by Mason, it is at best an example of "limited hysteresis" with numerous additional problems. A simple way to improve asymptotic convergence to zero and thereby eliminate the singularity at $K(0)$ is to multiply the impulse response by an exponential. Thus we examine F2,

$$\text{UnitStep}[t]\exp[-t/4]/t. \tag{27}$$

Its Fourier transform is

$$\frac{1}{\sqrt{2\pi}}\left(-\gamma + i\arctan[4\omega] + \log[4] - \frac{1}{2}\log[1 + 16\omega^2]\right). \tag{28}$$

A plot of the real and imaginary parts of the Fourier transform are given in Fig. 1. The shape of the transforms is typical of this family of relatives to $1/t$, and the long negative real part of $K(\omega)$ is still present. A number of other functions similar to $1/t$ have transforms similar to those of F1 and F2. Notably, they have a flat imaginary part at high frequency. These are given in Table I. The time domain character of some of these functions is given in Fig. 2.

Many of the practical issues with the previous functions (F1–F7) can be favorably resolved by removing the singularity of the impulse response at $t = 0$. For example,

H1: The function

$$\text{UnitStep}[t]\text{csch}[t + \varepsilon] \tag{29}$$

has the transform

$$\frac{i\mathbf{e}^{-\varepsilon}\left(\sqrt{\frac{2}{\pi}}\right)\text{Hypergeometric2F1}\left[1, -\frac{1}{2}i(i+\omega), -\frac{1}{2}i(3i+\omega), \mathbf{e}^{-2\varepsilon}\right]}{(i+\omega)} \tag{30}$$

and for the case of $\varepsilon = 1/100\,000$, this transform is shown in Figs. 3(a) and 3(b) over different frequency ranges. The real part $K(\omega)$ cannot be a constant; however, it is positive and has a very slight decay over any octave from $\omega > 2$. This function is labeled highpass in the sense that $K(\omega)$ and $H(\omega)$ are rapidly varying until $\omega > 2$.

Of course for earthquake or other work with lower frequency components the response can be scaled since $\Im(at) = (1/a)F(\omega/a)$, so $\omega_{min}$ can be adjusted as needed. Furthermore, in principle we can add a constant $K_0$ such that the real part of $(K_0 + K(\omega) + jH)$ will be positive between $\omega_{min} < \omega < \omega_{max}$. This provides a highpass function that

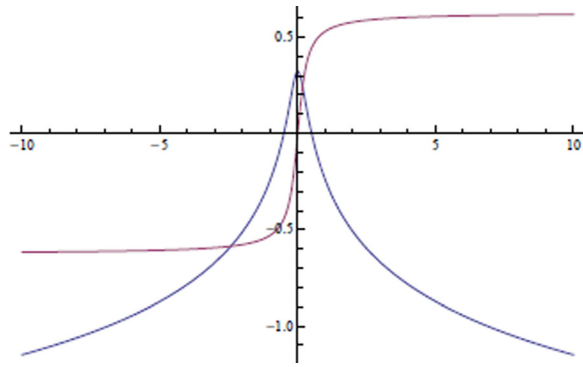Kevin J. Parker: Real and causal hysteresis elements

FIG. 1. (Color online) The frequency domain transfer function of highpass hysteresis function F2. $K(\omega)$ is real and even, $H(\omega)$ is odd and imaginary. The magnitudes of $K$ and $H$ are shown over the frequency range $-10 < \omega < 10$. The imaginary part, $H$, is relatively constant for $\omega > 2$ to infinity. Under certain conditions, this results in a constant loss per cycle, the hysteresis effect, for those frequencies. However, the negative values of $K(\omega)$ are not applicable to passive, non-resonant media.
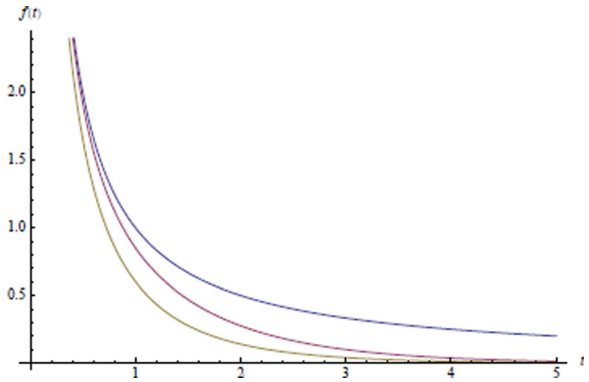


FIG. 2. (Color online) The functions $1/t$ (the outermost function), $\mathrm{csch}[t]$, and $K_1[t]$ (the innermost function) are shown over a range of $0 < t < 5$. These are representative of functions F1–F7 in Table I which are similar in that they have a singularity at $t = 0$ and also their transforms approach a flat imaginary component for high frequencies.

approaches the strict hysteresis criterion. In practice, any of the functions F1–F7 can be improved by replacing UnitStep$[t]f(t)$ with UnitStep$[t]f(t + \varepsilon)$, where $\varepsilon$ is small but $>0$. The closed form transforms are lengthy, however, and will not be reproduced here.

Next, examples of lowpass hysteresis functions are given.
L1:

$$\frac{11}{2}\left[\mathrm{MeijerG}\left[\left\{\left\{\frac{3}{4}\right\},\{\}\right\}\left\{\left\{\frac{1}{4},\frac{3}{4},\frac{3}{4}\right\},\right.\right.\right.$$
$$\left.\left.\left.\left\{0,\frac{1}{2}\right\}\right\},\frac{(11t)^4}{256}\right]\mathrm{UnitStep}[t]\right],\tag{31}$$

has the Fourier transform

$$-11^2\frac{\left(\pi\omega^2 - 11^2\log\big(|\omega|^4/11^4\big) - (2\times11^2)i\pi\,\mathrm{Sign}[\omega]\right)}{4\pi(11^4 + \omega^4)}.\tag{32}$$

The plot of the real and imaginary components is given in Fig. 4. The impulse response is given in Fig. 5. The slow asymptotic decay as $t \rightarrow \infty$ leads to singularity of $K(\omega)$ as $\omega \rightarrow 0$, limiting its value at extremely low frequencies.

L2: The function

TABLE I. Some causal functions and their Fourier transforms that approach limited highpass hysteresis.

| | |
|---|---|
| F1 | $(1/t)\mathrm{UnitStep}[t]$ |
| | Fourier transform: $\dfrac{-2\gamma - 2\log[\mathrm{Abs}[\omega]] + i\pi\,\mathrm{Sign}[\omega]}{2\sqrt{2\pi}}$ |
| F2 | $\mathrm{UnitStep}[t]\exp[-t/4]/t$ |
| | Fourier transform: $\dfrac{1}{\sqrt{2\pi}}\left(-\gamma + i\arctan[4\omega] + \log[4] - \dfrac{1}{2}\log[1 + 16\omega^2]\right)$ |
| F3 | $\mathrm{csch}[t]\mathrm{UnitStep}[t]$ |
| | Fourier transform: $\dfrac{1}{2\sqrt{2\pi}}\left(-\mathrm{HarmonicNumber}\left[-\dfrac{1}{2}-\dfrac{i\omega}{2}\right] - \mathrm{HarmonicNumber}\left[\dfrac{1}{2}i(i+\omega)\right] + i\pi\tanh\left[\dfrac{\pi\omega}{2}\right]\right)$ |
| F4 | $\exp[-(t^2)/4] * (1/t) * \mathrm{UnitStep}[t]$ |
| | Fourier transform: $\dfrac{1}{\sqrt{2\pi}}\left(-\dfrac{\gamma}{2} + \dfrac{1}{2}i\pi\mathrm{erf}[\omega] - \omega^2\mathrm{HypergeometricPFQ}\left[\{1,1\},\left\{\dfrac{3}{2},2\right\},-\omega^2\right] + \log[2]\right)$ |
| F5 | $\sqrt{\dfrac{2}{\pi}}K_1[t]\mathrm{UnitStep}[t]$, where $K_1[t]$ is the modified Bessel function of first order. |
| | Fourier transform: $\dfrac{1}{\pi}\left(-\gamma + \dfrac{i\pi\omega}{2\sqrt{1+\omega^2}} - \dfrac{\mathrm{Abs}[\omega]\mathrm{arcsinh}[\mathrm{Abs}[\omega]]}{\sqrt{1+\omega^2}} + \log[2]\right)$. A plot of the real and imaginary parts of the Fourier transform are given in Fig. 2. |
| F6 | $\begin{cases} 1/t & 0 \leq t \leq 1 \\ 0 & \text{elsewhere} \end{cases}$ |
| | Fourier transform: $\dfrac{1}{\sqrt{2\pi}}[\mathrm{Ci}[\omega] + i\mathrm{Si}[\omega]]$, where $\mathrm{Ci}[\omega]$ is the cosine integral function and $\mathrm{Si}[\omega]$ is the sine integral function. This imaginary part ripples as the $\mathrm{Si}[\omega]$ function, but these converge to a few percent of steady value for $\omega > 50$. The real part has a negative singularity at $\omega = 0$, however. |
| F7 | $\left(\dfrac{1}{t(4+t^2)}\right)\mathrm{UnitStep}[t]$ |
| | Fourier transform: F7 has a Fourier transform with many terms. The imaginary part has an arctan shape that is flat from $|\omega| > 2$. |

$$\frac{\left(\sin\left[\frac{\omega_0 t}{2}\right]\right)^2}{t} \text{UnitStep}[t] \tag{33}$$

has the Fourier transform

$$\frac{1}{8\sqrt{2\pi}}\left(\begin{array}{c} 2\log[\text{Abs}[-\omega_0 + \omega]] - 4\log[\text{Abs}[\omega]] + 2\log[\text{Abs}[\omega_0 + \omega]] \\ -i\pi\,\text{Sign}[-\omega_0 + \omega] + 2i\pi\,\text{Sign}[\omega] - i\pi\,\text{Sign}[\omega_0 + \omega] \end{array}\right) \tag{34}$$

with a constant $H$ from $0 \leq \omega \leq \omega_0$. The impulse response begins at 0 (unlike the highpass examples), and oscillates around a $1/t$ decay while remaining positive. However, this function also has a singularity at $K(0)$. This can be mediated [resulting in finite $K(0)$] by increasing the decay of the impulse response. Hence the function,

L3:

$$\frac{\left(\sin\left[\frac{\omega_0 t}{2}\right]\right)^2}{t}\exp[-t/\tau] * \text{UnitStep}[t], \tag{35}$$

has an improved Fourier transform with the real and imaginary parts graphed in Fig. 6 for parameters $\omega_0 = 10$ and $\tau = 10$.
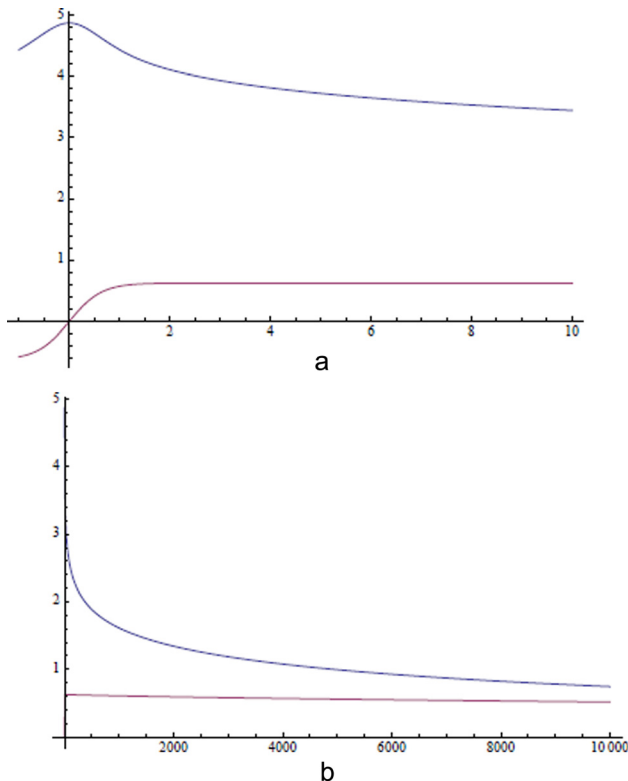
a

b

FIG. 3. (Color online) The frequency domain transfer function of the highpass hysteresis function H1, which is based on a $\text{csch}[t + \varepsilon]\text{UnitStep}[t]$ function in the time domain. The transfer function is shown for a particular value of $\varepsilon = 1/100\,000$ s. In (a) are the real and imaginary parts vs frequency, demonstrating a nearly constant imaginary part (lower) and slightly decreasing real part from 4–10 radians/s. In (b) is the transfer function over a greater frequency range, $0 \leq \omega \leq 10\,000$, showing slowly varying behavior within octaves up to 10 000 radians/s.

Finally, we examine bandpass behavior,
B1: The bandpass causal hysteretic function

$$\frac{\sqrt{\frac{2}{\pi}}(\cos[\omega_{\min}t] - \cos[\omega_{\max}t])\text{UnitStep}[t]}{t} \tag{36}$$

has the Fourier transform

$$\begin{aligned}\frac{1}{4\pi}\big(&\log[(\omega - \omega_{\max})^2(\omega + \omega_{\max})^2] \\ &- \log[(\omega - \omega_{\min})^2(\omega + \omega_{\min})^2] \\ &+ i\pi\big(\text{Sign}[\omega - \omega_{\max}] + \text{Sign}[\omega - \omega_{\min}] \\ &+ \text{Sign}[\omega + \omega_{\max}] + \text{Sign}[\omega + \omega_{\min}]\big)\big).\end{aligned} \tag{37}$$

The frequency domain real and imaginary plots are given in Fig. 7 for the parameters $\omega_{\min} = 2$; $\omega_{\max} = 9$. The corresponding impulse response is shown in Fig. 8. The severe cutoff nature of the frequency domain imaginary component leads to prominent oscillations (Gibbs phenomenon) in the impulse response, and also to singularities in the real part, $K(\omega)$, at $\omega_{\min}$ and $\omega_{\max}$.

Nonetheless, bandpass function B1 has remarkable properties. Inside the hysteretic band, the response of this element to an input $S(t) = \sin(\omega_o t)\text{UnitStep}(t)$ is, after a short startup transient, the expected hysteretic phase shift as shown in Fig. 9 for the parameter $\omega_0 = 5$ inside the band $\omega_{\min} = 2$, $\omega_{\max} = 9$. However, given the sinusoidal input
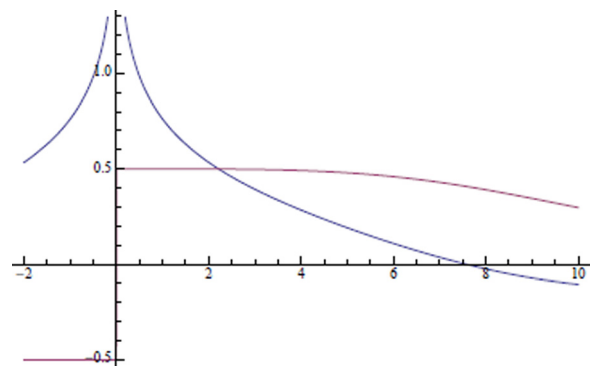
FIG. 4. (Color online) The frequency domain transfer function of lowpass hysteresis function L1. $K(\omega)$ is real and even, $H(\omega)$ is odd and imaginary. The magnitudes of $K$ and $H$ are shown over the frequency range $-2 < \omega < 10$. The imaginary part, $H$, is relatively constant for $\omega = 0$–5. At higher frequencies, $H$ drops off slowly and tends to zero. This would correspond to an observation of the hysteresis effect at lower frequencies.
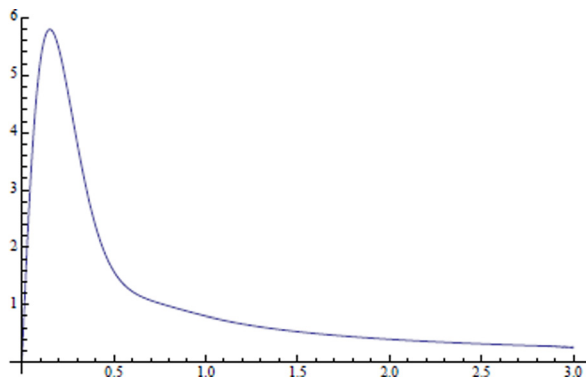
Kevin J. Parker: Real and causal hysteresis elements

FIG. 5. (Color online) The time domain impulse response of lowpass hysteresis function L1. This function begins at zero at $t = 0$, unlike the highpass functions which exhibit a singularity at $t = 0$.
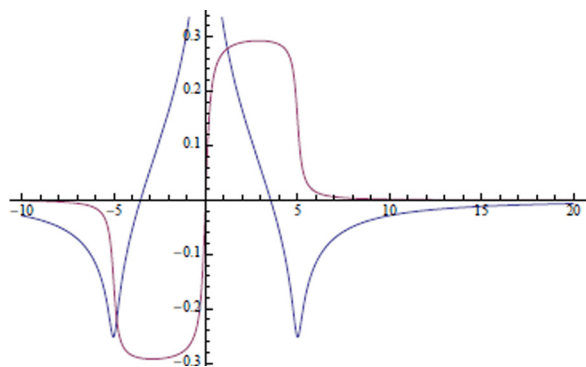


FIG. 6. (Color online) The frequency domain transfer function of lowpass hysteresis function L3, with the parameters $\omega_0 = 10$ and $\tau = 10$. $K(\omega)$ is real and even, $H(\omega)$ is odd and imaginary. The magnitudes of $K$ and $H$ are shown over the frequency range $-10 < \omega < 20$. The imaginary part, $H$, is relatively constant below $\omega = 5$, except at the transition around $\omega = 0$.
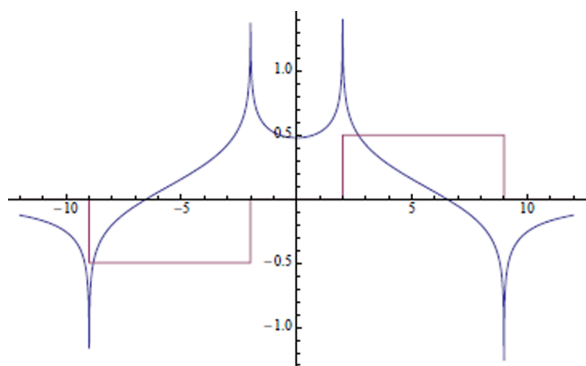


FIG. 7. (Color online) The frequency domain transfer function of bandpass hysteresis function B1, with the parameters $\omega_{\min} = 2$ and $\omega_{\max} = 9$. $K(\omega)$ is real and even, $H(\omega)$ is odd and imaginary. The magnitudes of $K$ and $H$ are shown over the frequency range $-10 < \omega < 10$. The imaginary part, $H$, is constant from $2 < \omega < 9$. Inside this band, the function exhibits hysteresis. However, outside this band the function has zero phase shift.
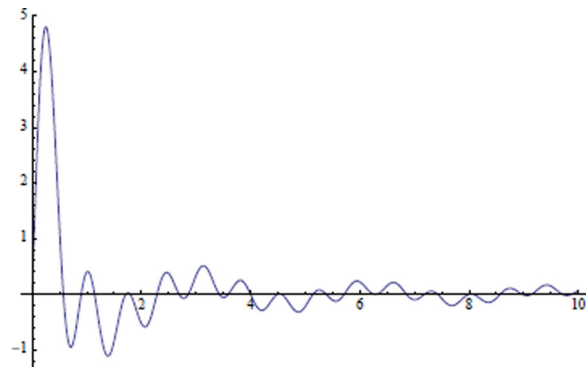


FIG. 8. (Color online) The corresponding time domain impulse response of bandpass hysteresis function B1. This function begins at zero at $t = 0$ and exhibits oscillations that are pronounced due to the severe sharp transitions in the frequency domain (see Fig. 7).

with $\omega_0$ outside of the band, after a short startup transient the element acts like a purely elastic material as shown in Fig. 10 for $\omega_0 = 1$ (below the hysteretic band of this example).

In practical systems, such sharp cutoffs are unrealistic, so smoother bandpass functions can be applied. Many bandpass shapes are discussed in the field of signal processing. Some smooth shapes that include functions already seen in the highpass examples include the forms

$$\left\{ \mathrm{erf}[\omega - \omega_{\min}] - \mathrm{erf}[\omega - \omega_{\max}] \right\} \tag{38}$$

or

$$\left\{ \arctan[\omega - \omega_{\min}] - \arctan[\omega - \omega_{\max}] \right\} \quad \text{for} \quad \omega > 0, \tag{39}$$

and these have closed form inverse transforms. A bandpass polynomial of the type

$$\frac{(\Delta\omega)^{2n}}{(\omega - \omega_0)^{2n} + (\Delta\omega)^{2n}} \quad \text{for} \quad \omega > 0 \tag{40}$$

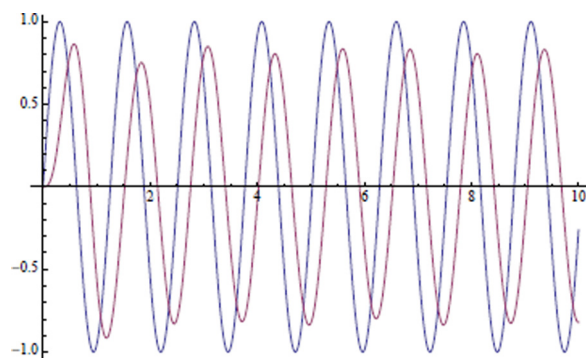is smooth, and has a closed form transform for $n = 1$ or $2$.



FIG. 9. (Color online) The input sine wave (leading) and output (lagging) of bandpass hysteresis function B1 for input frequency of 5, which lies within the hysteresis band. After a short transient, the system produces a phase lag with respect to the input.
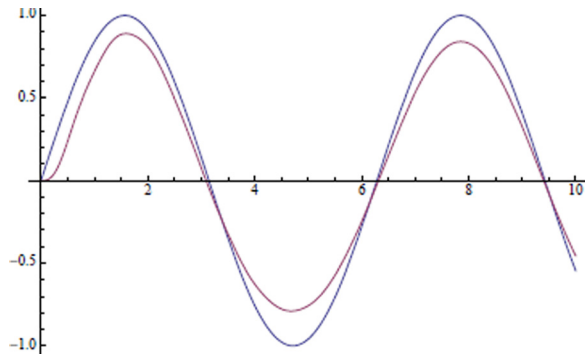
FIG. 10. (Color online) The input sine wave (larger) and output (smaller) of bandpass hysteresis function B1 for input frequency of 1, which is below the hysteresis band. After a short transient, the system response is essentially an in-phase copy of the input. This would resemble a lossless elastic element at low and high frequencies outside of the hysteresis band.

## IV. DISCUSSION AND CONCLUSIONS

There is a large family of real, causal functions that come close to the requirement of approximately constant real and imaginary transforms over some observable frequency range. Examples are provided and these do not represent an exhaustive and complete set. Rather, they are offered to illustrate the scope and range of real and causal hysteretic functions. This family can be conveniently grouped into subcategories of highpass, lowpass, and bandpass hysteretic causal functions depending on the nature of the frequency range that is covered. The impulse response of the highpass functions tend to resemble the $1/t$ function with a singularity at $t = 0+$. The lowpass functions have different impulse responses without necessarily having a singularity at $t = 0+$. Bandpass functions tend to have an oscillatory impulse response. All satisfy the key approximation of Eq. (10) (or "limited hysteresis") over a specified frequency range, and all have causal and real impulse responses, thus are compatible with practical realizations in nature and in the laboratory. A necessary result of causality constraints is that the real part of the transfer function, $K(\omega)$, will not be constant if $H$ is constant. However, $K(\omega)$ can vary slowly [or $K(\omega) + K_0$ even more slowly] over a specified frequency range, approaching the ideal, or "strict hysteresis" behavior.

A limitation of this study is that there is no attempt to decide which of the family of functions is the most realistic for a given material and experimental condition. This requires case-by-case evaluation of the response of the material under investigation, although some theoretical considerations apply. For example, Makris and Zhang (2000) argue that the model of Biot (1958) of an infinite number of parallel Maxwell elements can, in the high frequency limit, be shown to yield a causal function with a real part given by a log[$\omega$] function and the imaginary part given by the Sign[$\omega$] function. Thus, combinations of basic elements (or distributions of basic elements) under different models may be demonstrated to produce specific functions from the family of highpass, lowpass, and bandpass causal hysteresis elements. This phenomenological modeling approach itself is limited to supporting, but not "proving" the suitability of one member of the family over any other. Another approach would be to measure the impulse response or step response of a discrete element at the highest possible sampling rate (and duration) so as to determine a curve fit over the widest possible frequency range. In practice, noise and baseline drift will contaminate measurements and thereby can limit our ability to support one member of the family over others. Some forms of $K(\omega) + jH(\omega)$ and their impulse responses are unlikely to be seen in nature. For instance, the impulse response of highpass function H5 has a sharp cutoff to zero in the time domain at $t = 1$ s. Some other candidates have a $K(\omega)$ singularity at $\omega = 0$, implying that the material stiffness must increase sharply as frequency approaches zero. It is unlikely that passive common materials possess these exotic properties. The more smooth and slowly varying forms of $K(\omega)$ or $K_0 + K(\omega)$ are more likely to fit passive materials. Active damping systems could be designed to approach the more complicated transfer functions, however.

These considerations emphasize the need for the modeling of hysteresis starting from molecular or macromolecular phenomenon. This modeling from fundamentals is an important task for future research.

These results should be helpful over a wide range of endeavors where hysteresis has been found to play a role and where real, causal analytical models are required to predict wave propagation and the response of materials and structures.

Biot, M. A. (**1958**). "Linear thermodynamics and the mechanics of solids," in *American Society of Mechanical Engineers Third U.S. National Congress of Applied Mathematics*, pp. 1–18.

Blackstock, D. T. (**2000**). *Fundamentals of Physical Acoustics* (Wiley, New York), Chap. 9.

Bracewell, R. N. (**1965**). *The Fourier Transform and its Applications* (McGraw-Hill, New York), pp. 267, 411–426.

Carstensen, E. L., and Parker, K. J. (**2014**). "Physical models of tissue in shear fields," Ultrasound Med. Biol. **40**, 655–674.

Caughey, T. K. (**1962**). "Vibration of dynamic systems with linear hysteretic damping (linear theory)," in *4th U.S. National Congress of Applied Mechanics*, American Society of Mechanical Engineering, pp. 87–97.

Crandall, S. H. (**1963**). "Dynamic response of systems with structural damping," in *Air, Space and Instruments*, edited by S. Lees (McGraw-Hill, New York), pp. 183–193.

Crandall, S. H. (**1970**). "The role of damping in vibration theory," J. Sound Vib. **11**, 3–18.

Inaudi, J. A., and Kelly, J. M. (**1995**). "Linear hysteretic damping and the Hilbert transform," J. Eng. Mech. **121**, 626–632.

Kimball, A. L., and Lovell, D. E. (**1927**). "Internal friction in solids," Phys. Rev. **30**, 948–959.

Makris, N., and Zhang, J. (**2000**). "Time-domain viscoelastic analysis of earth structures," Earthq. Eng. Struct. D **29**, 745–768.

Mason, W. P. (**1950**). "Hysteresis losses in solid materials," in *Piezoelectric Crystals and their Application in Ultrasonics* (Van Nostrand, New York), p. 482.

Mason, W. P., and McSkimin, H. J. (**1947**). "Attenuation and scattering of high frequency sound waves in metals and glass," J. Acoust. Soc. Am. **19**, 464–473.

Nachman, A. I., Smith, J. F., and Waag, R. C. (**1990**). "An equation for acoustic propagation in inhomogeneous-media with relaxation losses," J. Acoust. Soc. Am. **88**, 1584–1595.

Nakamura, N. (**2007**). "Practical causal hysteretic damping," Earthq. Eng. Struct. D **36**, 597–617.

Nasholm, S. P., and Holm, S. (**2011**). "Linking multiple relaxation, power-law attenuation, and fractional wave equations," J. Acoust. Soc. Am. **130**, 3038–3045.

Papoulis, A. (**1987**). *The Fourier Integral and its Applications* (McGraw-Hill, New York), p. 11.

Szabo, T. L., and Wu, J. (**2000**). "A model for longitudinal and shear wave propagation in viscoelastic media," J. Acoust. Soc. Am. **107**, 2437–2446.

Theodorsen, T., and Garrick, I. E. (**1940**). "Mechanism of flutter, a theoretical and experimental investigation of the flutter problem," NACA Rep. **685**, 101–146.

Wegel, R. L., and Walther, H. (**1935**). "Internal dissipation in solids for small cyclic strains," Physics **6**, 141–157.